Magnetic Microactuators Based on Polymer Magnets

Laure K. Lagorce, Oliver Brand, *Member, IEEE*, and Mark G. Allen, *Member, IEEE*

Abstract—Integrated permanent magnet microactuators have been fabricated using micromachined polymer magnets. The hard magnetic material utilized is a polymer composite, consisting of magnetically hard ceramic ferrite powder imbedded in a commercial epoxy resin to a volume loading of 80%. The magnets have the form of thin disks approximately 4 mm in diameter and 90 μm in thickness. These disks have been magnetized in the thickness direction, and even in this geometrically unfavorable direction showed typical permanent magnet behavior with an intrinsic coercivity H_{ci} of 4000 Oe (320 kA/m) and a residual induction B_r of 600 Gauss (60 mT). Cantilever beam-type magnetic actuators carrying a screen-printed disk magnet on their free ends have been fabricated on an epoxy board. A planar coil on the opposite side of the substrate is used to drive the beams vertically. The actuators exhibit hard magnetic behavior allowing both attraction and repulsion by reversing the current direction. Static and dynamic testing of the magnetic actuators have been performed. The experimental data are compared with theoretical results obtained from both finite element simulations and analytical models. Good agreement is obtained between simulation and experiment. [273]

Index Terms—Magnetic, microactuator, micromachined, permanent magnet, polymer magnet, simulation.

I. INTRODUCTION

RECENTLY, there has been much interest in magnetic microactuators [1]–[13]. Compared to electrostatic actuators, electromagnetic actuators typically can be operated at substantially smaller voltages but might require larger driving currents. It has been shown that electromagnetic forces have the potential to generate large deflections [14].

Most of the magnetic microactuators developed so far are based on the variable reluctance principle and utilize soft magnetic materials [1]–[8]. However, hard magnetic materials are also desirable actuator components due to their favorable scaling [15] and the resulting potential for larger forces and larger deflections, applicable to milli-scale actuators. Permanent magnet microactuators have been previously demonstrated either using hybrid assembled, commercially available permanent magnets [9]–[11], or using electroplated CoNiMnP permanent magnets [12].

Previously, we demonstrated micromachined permanent magnets consisting of magnetic strontium ferrite powder imbedded in a polyimide matrix [13]. The polymer magnets can be processed using, e.g., standard screen-printing techniques. Therefore, fully integrated magnets with thicknesses up to several millimeters can be fabricated by a low-temperature processing method.

The purpose of this paper is to demonstrate how these polymer magnets can be used in magnetic microactuators and to illustrate typical analysis schemes for microactuators made from these materials. The work describes the fabrication and characterization of a simple magnetic actuator based on an electroplated copper cantilever beam with a polymer magnet integrated on its end. In contrast to the work presented in [13], an epoxy matrix has been utilized for the polymer magnets to further reduce the processing temperature. This reduced processing temperature makes it possible to construct the microactuators on low-cost copper-clad printed wiring boards, which allows micromachining to take place in or on the package of the MEMS system. Alternatively, if desired, the materials are also silicon-compatible. The experimental results are compared with theoretical results obtained from both finite element (FE) simulations and analytical models.

II. PERMANENT MAGNET POLYMER COMPOSITE

The permanent magnets used in this work are composed of strontium ferrite powder (with a grain size ranging from 1.15 to 1.5 μm) produced by Hoosier Magnetics and an epoxy resin produced by Shell. The polymer matrix consists of a bisphenol-A-based epoxy resin diluted with cresylglycidyl ether. An aliphatic amidoamine is used as a curing agent. In contrast to the previously reported polymer magnets [13], which used a polyimide matrix, the above epoxy matrix has been chosen in this work in order to reduce the maximum processing temperature. The epoxy resin was cured at 80 °C for 2 h. The reduced processing temperatures allow for more processing flexibility, e.g., the use of photoresist sacrificial layers and low-cost, low-temperature epoxy board substrates for the microactuator fabrication. Both epoxy board substrates and photoresist sacrificial layers are incompatible with the cure temperature (300 °C) of the polyimide used in [13]. However, if process temperature is not a limitation, the superior mechanical properties of the polymer magnets in [13] may be desirable.

The polymer magnet composites were prepared as described in [13]: the desired concentration of strontium ferrite powder is mixed with the epoxy using a ball mill rotating at 4–5 rpm for 72 h. After the curing agent is added, the epoxy magnets can be deposited and patterned using screen-printing

L. K. Lagorce was with the School of Electrical and Computer Engineering Microelectronics Research Center, Georgia Institute of Technology, Atlanta, GA 30332-0269 USA. She is now with the Centre d'Elaboration de Materiaux et d'Etudes Structurales (CEMES-CNRS), Toulouse, France.

O. Brand was with the School of Electrical and Computer Engineering Microelectronics Research Center, Georgia Institute of Technology, Atlanta, GA 30332-0269 USA. He is now with the Physical Electronics Laboratory, Swiss Federal Institute of Technology (ETH), Zurich, Switzerland.

M. G. Allen is with the School of Electrical and Computer Engineering Microelectronics Research Center, Georgia Institute of Technology, Atlanta, GA 30332-0269 USA (e-mail: mallen@ee.gatech.edu).
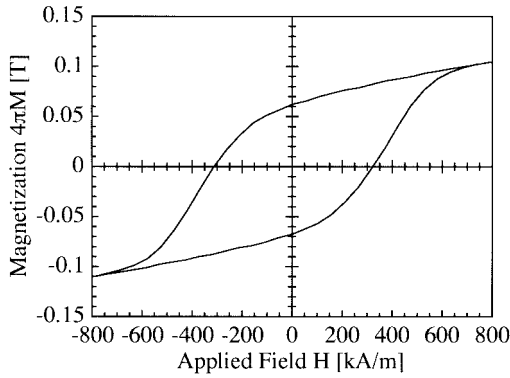
Fig. 1. 4πM-H curve for an epoxy-ferrite magnet (80 vol% strontium ferrite concentration) with 90 μm thickness magnetized in the thickness direction.

Fig. 2. Schematic view of the cantilever beam microactuator.

techniques, resulting in magnets with thicknesses ranging from hundreds of micrometers up to several millimeters. After screen-printing, the magnets are cured at 80 °C for 2 h and, finally, magnetized in the desired direction.

In this work, circular magnets with a thickness of approximately 90 μm and a diameter of 2–4 mm were investigated. The polymer magnets were magnetized in the thickness direction to achieve vertical actuation (out-of-plane actuation) of the cantilever beam structures. The magnetic properties of the thin disc magnets magnetized in the thickness direction were measured using a vibrating sample magnetometer (VSM). Fig. 1 shows the 4πM-H curve of a strontium ferrite-epoxy composite magnet (80 vol% strontium ferrite concentration) with a thickness and diameter of 90 μm and 4 mm, respectively, magnetized in thickness direction. This particular magnet exhibits an intrinsic coercivity H_{ci} and residual induction B_r of 4000 Oe (320 kA/m) and 600 Gauss (60 mT), respectively.

The results presented in [13] show a residual induction of the order of 3000 Gauss, but are obtained for samples magnetized in the thin-film plane. The polymer magnets used in this work are magnetized normal to the thin-film plane. The difference between both measurements can be explained by the influence of demagnetization effects [16], as applied to this geometrically unfavorable magnetization direction. The demagnetization factor and resulting demagnetization field are larger for a thin-film magnet magnetized in the thickness direction (i.e., normal to the film plane) than for the same magnet magnetized in the film plane, and the resultant effective residual induction is reduced due to this geometric effect.

III. PERMANENT MAGNET ACTUATORS

The basic structure of the fabricated cantilever beam microactuators is illustrated in Fig. 2. A polymer magnet magnetized in thickness direction is screen-printed onto the free end of a copper cantilever beam. On the other side of the substrate, a planar square coil produces the magnetic field gradient necessary for the actuation of the magnet. The vertical electromagnetic force F_z acting on a magnet with apparent magnetization M_z (corrected by the demagnetization effect) and volume V is given by [17]

$$F_z = M_z \int_V \frac{dH_z}{dz}\, dV \qquad (1)$$
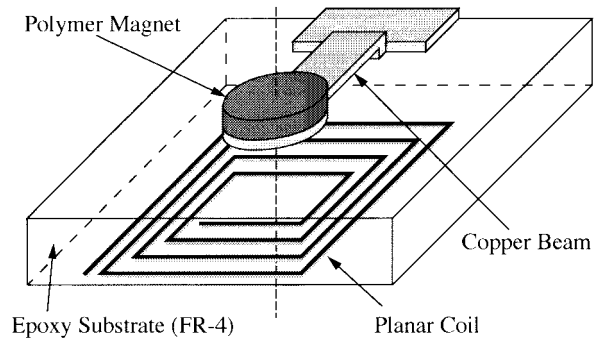
where H_z is the vertical component of the magnetic field produced by the planar coil. The expression of H_z produced by a square current loop can be obtained by integration of the Biot-Savart Law and has been derived in detail in [9]. To achieve a magnetic gradient, the center of the magnet must be placed outside the plane of the coil. The electromagnetic force is proportional to the volume of the magnet. Therefore, screen-printed magnets, in which thicknesses up to several millimeters are achievable, may be preferable to spin-cast polymer magnets. Thicker magnets would also help to reduce the demagnetization effect.

The static deflection δ of a cantilever beam, subject to a concentrated load F at its free end, is given by [18] (using small deflection theory)

$$\delta = \frac{FL^3}{3EI} \qquad (2)$$

where L, E, and I are the length of the beam, the Young's modulus, and the moment of inertia, respectively. For a cantilever beam with rectangular cross section, I is given by [18]

$$I = \frac{bh^3}{12} \qquad (3)$$

where b and h are the width and thickness of the beam, respectively. Using (1), (2), and (3), as well as the analytical expression of the magnetic field generated by a square coil [9], the expected deflections of the cantilever beam actuators can be calculated analytically.

In addition to the use of analytical models for the description of the magnetic actuator, finite element simulations using the general-purpose finite element software ANSYS (Version 5.2) have been performed, in order to obtain the static deflection as well as the resonance frequencies of the permanent magnet actuators. The static deflection of the cantilever beam with the permanent magnet at its tip is calculated in two steps. First, the force acting on the permanent magnet is calculated as a function of the distance between magnet and planar coil using a magnetic analysis. In a subsequent structural analysis, the deflection of the copper cantilever beam due to the magnetic force is simulated. Iterations are not required as long as the magnitude of the deflection of the cantilever beam is small compared to the spatial scale over which the magnetic force varies (this assumption will be verified in
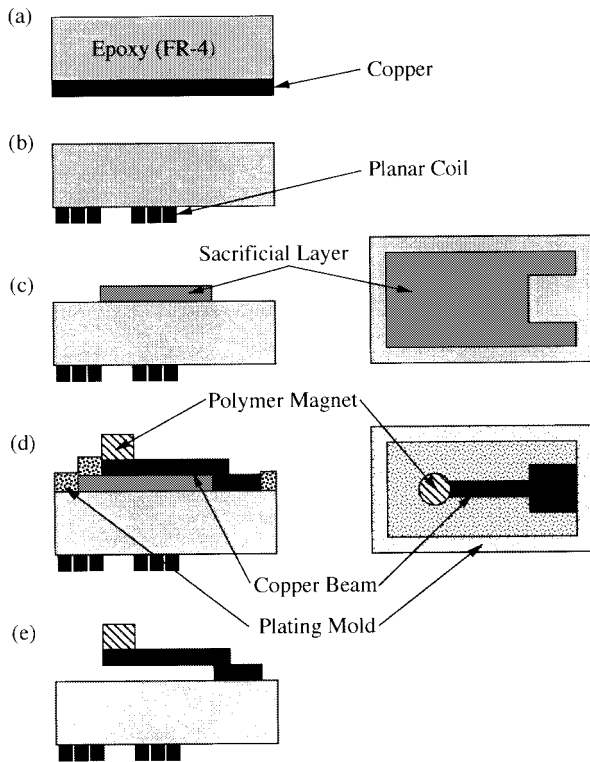
Fig. 3   (a)–(e) Fabrication sequence of the magnetic microactuators.

Fig. 4.   Photomicrograph of a fabricated microactuator.

the subsequent analysis). The resonance frequencies of the beam-type actuators are obtained in a single modal analysis.

IV. ACTUATOR FABRICATION

The permanent magnet microactuators were fabricated by combining standard micromachining techniques (such as sacrificial layer techniques) with process steps (e.g., electroplating, screen printing, and lamination) and materials (e.g., epoxy boards) adapted from the electronic packaging industry.

Fig. 3(a)–(e) shows a schematic of the fabrication process. The magnetic microactuators were fabricated on commercially available epoxy board (FR-4) substrates which had a copper-clad layer 20 μm in thickness laminated on one side. The coil structure was defined in this cladding layer using standard photolithography, followed by wet etching in a ferric chloride solution. The resulting 20-μm thick coil consists of 31 turns with a linewidth and spacing of 70 μm. The inner and outer side lengths of the coil were 4 and 12.4 mm, respectively.

After completion of the planar coil, the cantilever beam carrying the permanent magnet was fabricated on the other side of the substrate. First, a 35-μm thick photoresist sacrificial layer was spin-coated and patterned on the substrate. A Ti/Cu/Cr seed layer for the copper electroplating step was then deposited. A second photoresist layer was spun and patterned to serve as a mold for the electroplating of the copper cantilever beam. Next, the copper cantilever beam was electroplated in a standard copper-sulfate-based plating bath. After the electroplating step, the photoresist plating mold and the seed layer were removed and the 90-μm thick magnet was screen-printed onto the cantilever beam. After curing the epoxy magnet at 80 °C for 2 h, the magnets were exposed
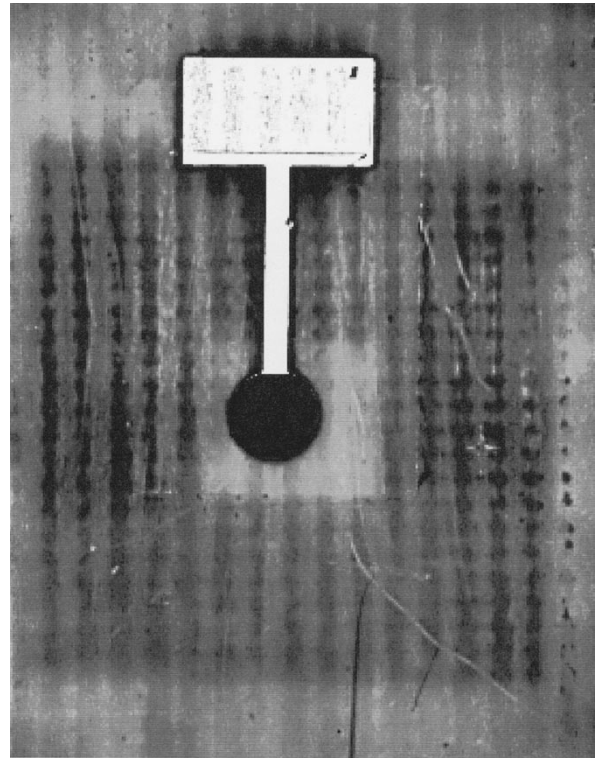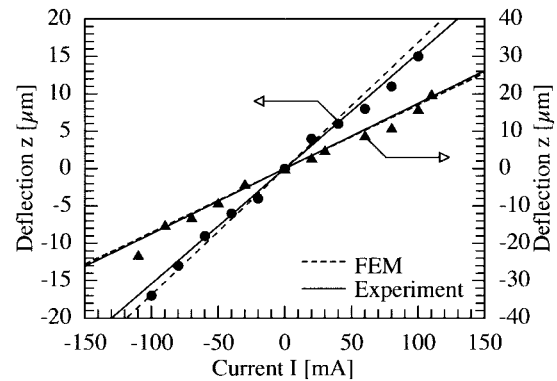
Fig. 5.   Static deflection of two different microactuators as a function of the driving current; circles: length 7 mm, width 1 mm, thickness 25 μm, magnet diameter 4 mm; triangles: length 5 mm, width 0.5 mm, thickness 11.5 μm, magnet diameter 2 mm.

to an external magnetic field for magnetization. Finally, the cantilever beam actuators were released by removing the sacrificial photoresist layer using acetone.

A photograph of a fabricated and released magnetic microactuator is shown in Fig. 4. The planar coil on the other side of the epoxy board can be seen as a shadow. Due to initial stress gradients, the copper beams bend upward. Depending on the device geometry, the actual spacing between the beam tip and the substrate varies between 160 and 400 μm.

V. EXPERIMENTAL RESULTS

A. Static Deflection of the Magnetic Actuators

The deflection of the cantilever beam actuators in the magnet center was measured as a function of the dc coil current using a microscope with height measurement capa-
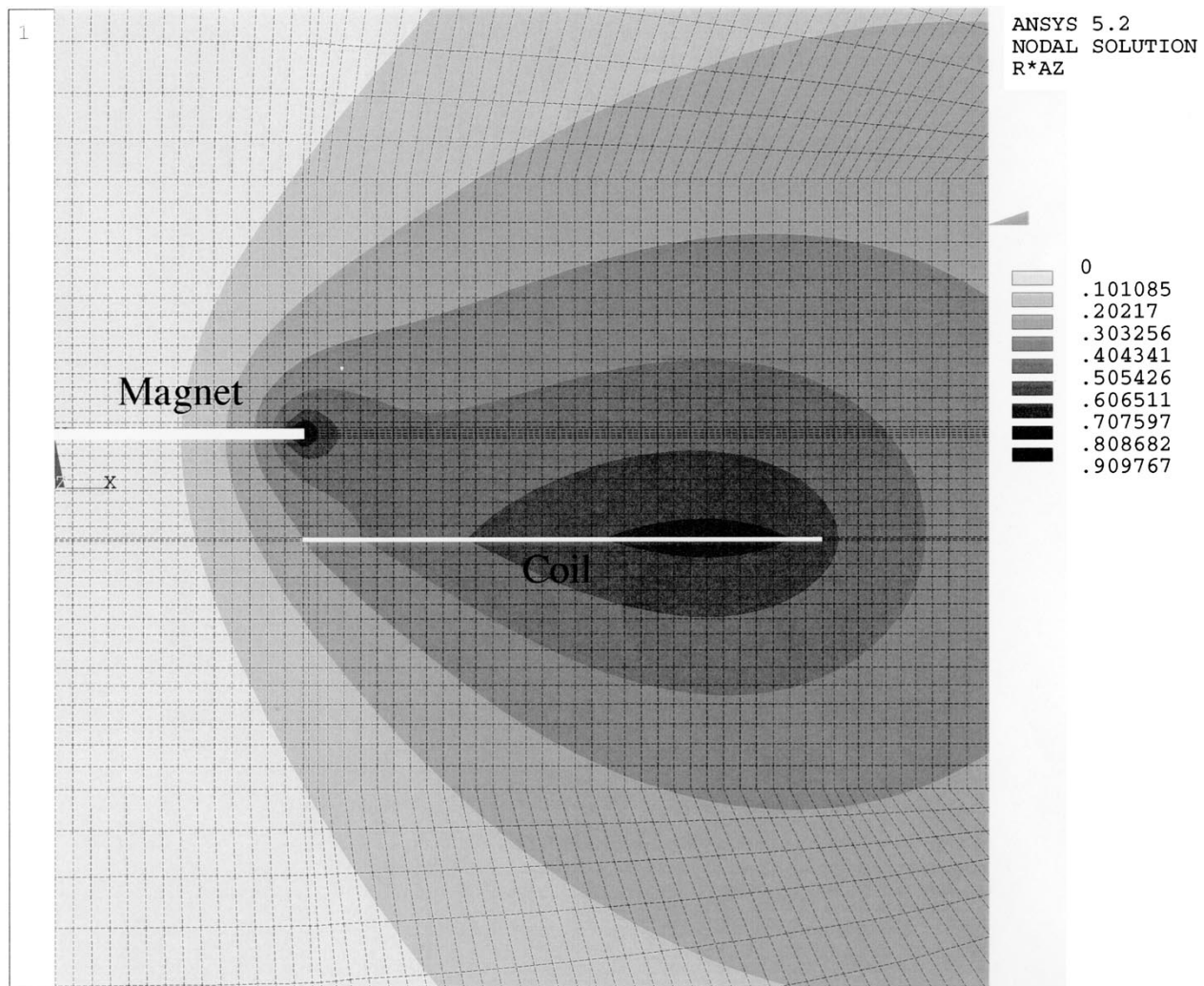
Fig. 6. Simulated vector potential A_z times radial coordinate r for a magnet with 4 mm diameter and 0.8 mm spacing between magnet and coil; the driving current is 100 mA.

bility. Fig. 5 shows the transverse deflection in the magnet center as a function of the driving current for two different device geometries: a) a 7-mm long, 1-mm wide, and 25-μm thick cantilever beam supporting a 90-μm thick epoxy magnet with 4 mm diameter; and b) a 5-mm long, 0.5-mm wide, and 11.5-μm thick cantilever beam supporting a 90-μm thick epoxy magnet with 2 mm diameter. As expected for a permanent magnet actuator, both attraction and repulsion of the permanent magnet can be achieved by reversing the current direction. Moreover, the deflections increase linearly with the driving current. For a driving current of 100 mA, the cantilever beam deflections are approximately 17 μm, i.e., much smaller than the beam length. Therefore, the experimental results can be compared with the deflections calculated from the small deflection theory [see (2)].

The static deflection of the magnetic actuators was simulated using the finite element program ANSYS. In a first step, the magnetic forces were calculated in a static magnetic analysis. The finite element model for the magnetic analysis consists of the disk magnet, the planar coil, and the surrounding air. The copper beam with $\mu_r = 1$ is simulated as air. Assuming a circular coil with a centered disk magnet above it, only a

simplified two-dimensional, axisymmetric magnetic problem was solved. In addition, the planar coil with 31 windings was approximated by a continuous copper ring of width equal to the total width of the 31-winding coil and carrying 31 times the current. This assumption certainly affects the magnetic field in the vicinity of the coil windings but far less so at the location of the permanent magnet. Since the magnetic field gradient generated by the coil at the location of the permanent magnet is the field of importance for the calculation of the actuation force, this approximation to the actual coil geometry was deemed acceptable.

Two-dimensional *eight-node magnetic solid elements* (PLANE53) were used to model the permanent magnet, the coil, and the surrounding air. In addition, two-dimensional four-node boundary elements (INFIN110) were used along the edges of the model (except along the symmetry axis) to simulate an infinite extension of the air surrounding the actuator. The magnetic properties of the permanent magnet as measured with the vibrating sample magnetometer (as shown in Fig. 1) were entered into the ANSYS model in form of a B-H table. This measured magnetization was assumed to apply to the entire volume of the magnet. The complete finite

TABLE I
SUMMARY OF EXPERIMENTAL AND THEORETICAL RESULTS

	Beam # 1 Length 7 mm Width 1 mm Thickness 25 µm Magnet Diameter 4 mm	Beam # 2 Length 5 mm Width 0.5 mm Thickness 11.5 µm Magnet Diameter 2 mm	Beam # 3 Length 6 mm Width 1 mm Thickness 19.5 µm Magnet Diameter 4 mm
Force F_z [µN] FEM	10	1.6	10
Force F_z [µN] Analytical Model	11	1.8	11
Deflection [µm] Experimental Results	15	16	34
Deflection [µm] FEM	17	18	25
Deflection [µm] Analytical Model	18	19	27
Resonance Frequency f_1[Hz] Experimental Results	41	45	30
Resonance Frequency f_1[Hz] FEM	43	39	37
Vibration Amplitude A [µm] Experimental Results	120	330	85

element model consists of approximately 5400 elements, each having one degree of freedom (the vector potential A_z).

As an example, Fig. 6 shows the vector potential A_z times the radius r created by a disk magnet with thickness and diameter of 90 µm and 4 mm, respectively, and the coil with 31 turns at a current $I = 100$ mA. The coil has an inner and outer radius of 2 and 6.2 mm, respectively. The distance between coil and magnet is 0.8 mm. The position of the planar coil and the magnet within the model are shown in Fig. 6 by the white lines. In an axisymmetric analysis, constant lines of $A_z \cdot r$ are parallel to the magnetic field vector B [19].

The force acting on the permanent magnet was calculated within the magnetic analysis using the magnetic virtual displacement (MVDI) loading [19] available in the ANSYS program. The achievable actuation forces were calculated as a function of the magnet dimensions and the distance d between coil and magnet. For the actuator configuration shown in Fig. 6 (polymer magnet: 90 µm thickness, 4 mm diameter; coil: 31 turns, 100 mA current, 2 mm inner radius, 6.2 mm outer radius; 0.8 mm spacing between coil and magnet), the ANSYS simulation gives a force $F_z = 9.8$ µN acting on the magnet in the direction parallel to the symmetry axis. Fig. 7 shows the actuation force F_z as a function of the distance d between coil and magnet for permanent magnets with different diameters for constant coil dimensions. As expected, the actuation force generally increases with increasing magnet diameter, i.e., increasing magnet volume. The magnetic force can be optimized for a particular magnet dimension by optimizing
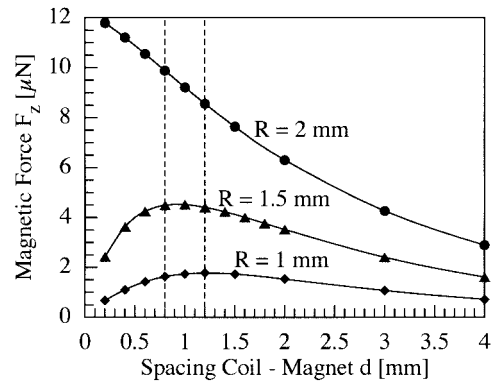
Fig. 7. Simulated actuation force F_z as a function of the distance between coil and magnet for different magnet sizes (coil dimension: 31 turns, 2 mm inner diameter, 6.2 mm outer diameter; magnet dimensions: 90 µm thickness).

the distance between coil and magnet. The optimal spacing shifts to smaller values for increasing magnet diameter. In the case of the magnet with 4 mm diameter, the maximum force is obtained at a spacing below 0.2 mm and is not shown in Fig. 7. Table I summarizes the magnetic forces obtained for different magnet dimensions for a coil-magnet spacing of 0.8 mm and compares the results of the FE simulations with the analytical results obtained from (1)–(3).

The static deflection of the cantilever beams due to the magnetic forces was calculated in a subsequent mechanical analysis. *Four-node structural shell elements* (SHELL143) were used to model the copper cantilever beam. The beam
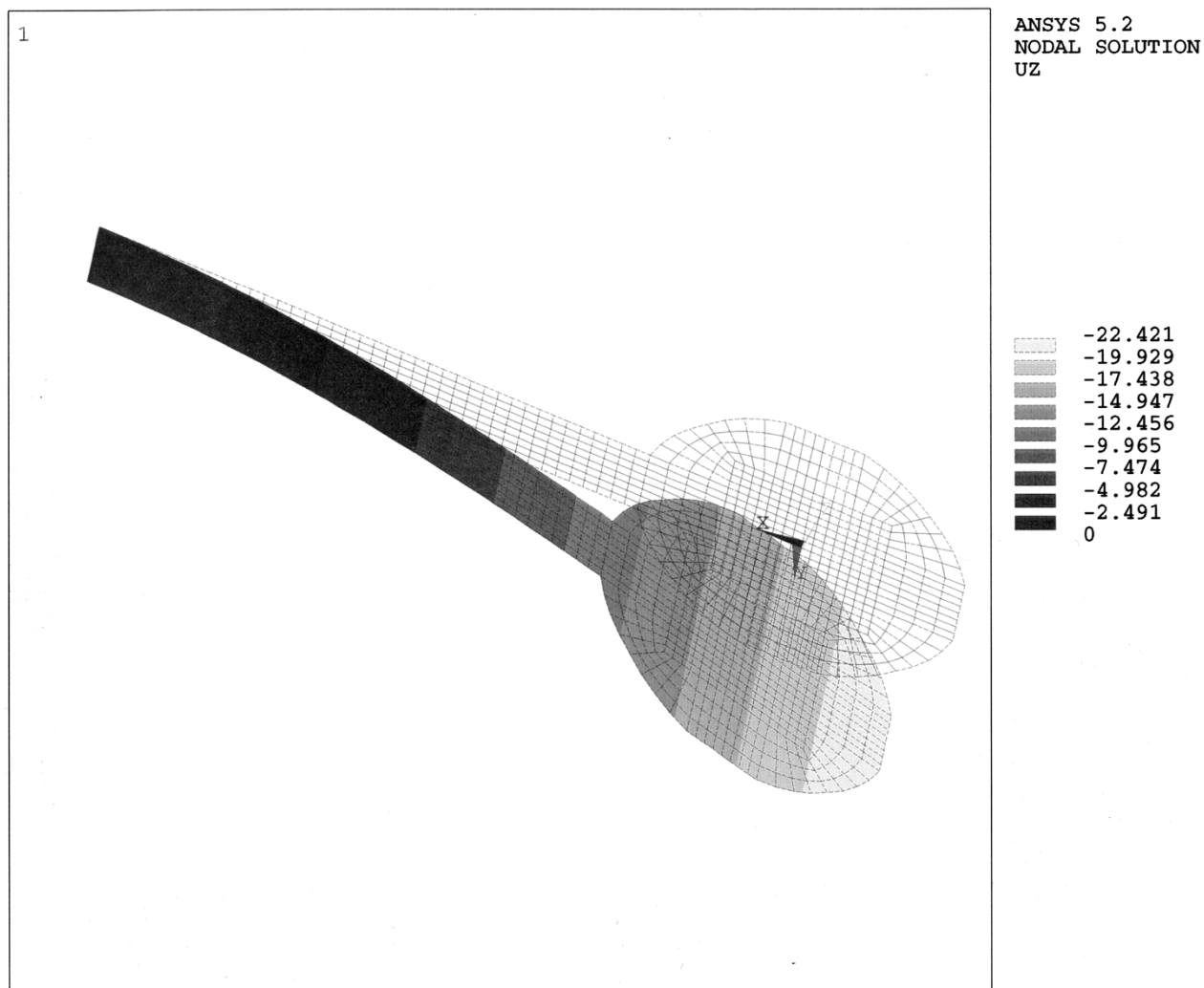
Fig. 8.   Simulated deflected beam shape for the 7-mm long, 1-mm wide, and 25-μm thick beam carrying a magnet with 4 mm diameter and 90 μm thickness.

was clamped along one end and the magnetic forces were applied as a constant pressure over the magnet area. The latter assumption is justified since the beam deflection is small compared to the scale over which the magnetic forces change (see Fig. 7). Fig. 7 also verifies the assumption that since the magnitude of the deflection of the cantilever beam is small compared to the spatial scale over which the magnetic force varies, iteration between force and position of the beam is not required. The mechanical properties of the electroplated copper structure were approximated by literature values found for bulk copper [18]: Young's modulus $E = 110$ GPa, Poisson ratio $\nu = 0.33$, and density $\rho = 8900$ kg/m^3.

Fig. 8 shows a picture of a deflected beam structure. For a 7-mm long, 25-μm high, and 1-mm wide beam, supporting a magnet of 4 mm diameter and 90 μm thickness, a 17-μm deflection of the magnet center was calculated for a 0.8-mm spacing between coil and magnet and a driving current of $I = 100$ mA (resulting driving force: $F_z = 9.8$ μN). The static deflections of the beam actuators simulated using ANSYS are shown in Fig. 5 as dashed lines. The simulation results are in good agreement with the experimental results. The deviations between theory and experiments might arise from, e.g., variations in the beam thickness and the magnet

thickness and differences between the mechanical properties of the electroplated copper and the bulk properties used in the simulations. Table I summarizes the simulated deflections for the three different actuator geometries and compares the results of the FEM with analytical results, from (2) and (3), as well as experimental results.

B. Dynamic Behavior of the Magnetic Actuators

In addition to the static deflection measurements, the resonance frequencies and vibration amplitudes of the cantilever beam actuators were measured. To this end, the actuators were driven by a sinusoidal ac current. The vibration amplitude was again measured using a microscope with height measurement capability. Fig. 9 shows the vibration amplitude in the magnet center as a function of the driving frequency for the 7-mm long, 1-mm wide, and 25-μm thick beam supporting a magnet with 4 mm diameter. For a driving current of 50 mA$_{\mathrm{rms}}$, a vibration amplitude of 120 μm was obtained at the fundamental resonance frequency of 41 Hz. From the 3-dB bandwidth at resonance, a quality factor of ten can be estimated. The smallest device tested (5-mm long, 0.5-mm wide, and 11.5-μm thick cantilever beam supporting a magnet with 2 mm diameter) exhibits vibration amplitudes of 330 μm
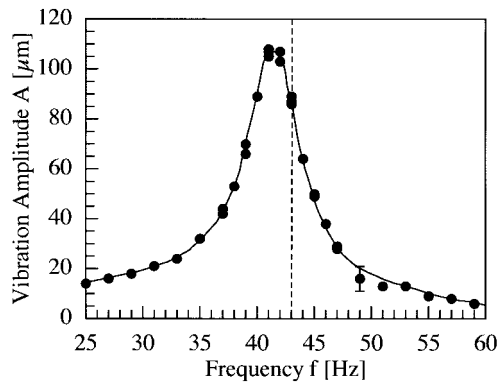
Fig. 9. Vibration amplitude A of the 7-mm long, 1-mm wide, and 25-μm thick beam carrying a magnet with 4 mm diameter as a function of the driving frequency.

at the fundamental resonance of 45 Hz at a driving current of 20 mA.

The resonance frequencies of the cantilever beam actuators were simulated using a modal analysis in ANSYS. Since the mass of the magnet must be included in the modal analysis, *eight-node layered shell elements* (SHELL91) were used to create the actuator model. The following material properties were assumed for the permanent magnet: Young's modulus $E = 17$ GPa (estimated from [13]) and density $\rho = 4300$ kg/m^3. For the beam shown in Fig. 8, the simulation predicts a resonance frequency of 43 Hz (dashed line in Fig. 9) which is in excellent agreement with the experimental result.

VI. CONCLUSION

This work demonstrates the feasibility of polymer-magnet-based integrated permanent magnet actuators which behave in a reproducible manner and which are well-described by analytical and finite element models. The hard magnetic microactuators have been realized using a low temperature, batch-fabrication-compatible process. The cantilever beam-type microactuators carry a screen-printed polymer magnet at their free end. The polymer magnet consists of strontium ferrite powder imbedded in an epoxy matrix. Vertical deflections of the microactuators are achieved using a planar driving coil on the opposite side of the substrate. The microactuators have been tested statically (deflections as a function of current) and dynamically (measurement of the resonant frequency). At the fundamental resonance frequency, large deflections in excess of 0.3 mm have been observed for driving currents as low as 20 mA. The experimental data are in good agreement with theoretical results obtained using either finite element analysis or analytical models using no fitted parameters. This allows for the future optimization of magnetic microactuators and the development of new types of permanent magnet sensors and actuators based on polymer magnets.

ACKNOWLEDGMENT

REFERENCES

[1] K. Yanagisawa, A. Tago, T. Ohkubo, and H. Kuwano, "Magnetic microactuator," in *Proc. 1991 IEEE MEMS Conf.*, Nara, Japan, pp. 120–124.
[2] C. H. Ahn and M. G. Allen, "A fully integrated surface micromachined magnetic microactuator with a multilevel meander magnetic core," *IEEE J. Microelectromech. Syst.*, vol. 2, no. 1, pp. 15–22, 1993.
[3] M. G. Allen, "Design, fabrication, and application of magnetic microactuators," in *Proc. 1994 Int. Symp. Micro Machine and Human Science*, Nagoya, Japan, 1994, p. 5.
[4] C. Liu, T. Tsao, Y. C. Tai, and C. M. Ho, "Surface micromachined magnetic actuators," in *Proc. 1994 IEEE MEMS Conf.*, Oiso, Japan, 1994, pp. 57–62.
[5] C. Liu, T. Tsao, Y. C. Tai, T. S. Leu, C. M. Ho, W. L. Tang, and D. Miu, "Out-of-plane permalloy magnetic actuators for delta-wing control," in *Proc. 1995 IEEE MEMS Conf.*, Amsterdam, Netherlands, 1995, pp. 7–12.
[6] C. Liu, T. Tsao, Y. C. Tai, W. Liu, P. Will, and C. M. Ho, "Micromachined permalloy magnetic actuator array for microrobotics assembly systems," in *Proc. 1995 Int. Conf. Solid-State Sensors and Actuators, Eurosensors IX*, Stockholm, Sweden, vol. 1, pp. 328–331, 1995.
[7] J. W. Judy, R. S. Muller, and H. H. Zappe, "Magnetic microactuation of polysilicon flexure structures," *IEEE J. Microelectromech. Syst.*, vol. 4, no. 4, pp. 162–169, 1995.
[8] W. P. Taylor, O. Brand, and M. G. Allen, "Fully integrated magnetically actuated micromachined relays," *IEEE J. Microelectromech. Syst.*, vol. 7, no. 2, pp. 181–191, 1998.
[9] B. Wagner and W. Benecke, "Microfabricated actuator with moving permanent magnet," in *Proc. 1991 IEEE MEMS Conf.*, Nara, Japan, 1991, pp. 27–32.
[10] B. Wagner, M. Kreutzer, and W. Benecke, "Permanent magnet micromotors on silicon substrates," *IEEE J. Microelectromech. Syst.*, vol. 2, no. 1, pp. 23–29, 1993.
[11] Y. Shinozawa, T. Abe, and T. Kondo, "A proportional microvalve using a bi-stable magnetic actuator," in *Proc. 1997 IEEE MEMS Conf.*, Nagoya, Japan, 1997, pp. 233–237.
[12] T. M. Liakopoulos, W. Zhang, and C. H. Ahn, "Electroplated thick CoNiMnP permanent magnet arrays for micromachined magnetic device applications," in *Proc. 1996 IEEE MEMS Conf.*, San Diego, 1996, pp. 79–84.
[13] L. K. Lagorce and M. G. Allen, "Magnetic and mechanical properties of micromachined strontium ferrite/polyimide composites," *IEEE J. Microelectromech. Syst.*, vol. 6, no. 4, pp. 307–312, 1997.
[14] I. J. Busch-Vishniac, "The case for magnetically driven microactuators," *Sensors and Actuators*, vol. A33, pp. 207–220, 1992.
[15] W. S. N. Trimmer, "Microrobots and micromechanical systems," *Sensors and Actuators*, vol. A19, pp. 267–287, 1989.
[16] B. D. Culliti, *Introduction to Magnetic Materials*. Reading, MA: Addison Wesley, 1972, pp. 49–61.
[17] B. Wagner and W. Benecke, "Magnetically driven microactuators: design considerations," *Microsystems Technologies 90*, H. Reichl, Ed. Berlin: Springer Verlag, 1990, p. 838.
[18] J. M. Gere and S. P. Timoshenko, *Mechanics of Materials*, 3rd ed. PWS-Kent, 1990.
[19] *ANSYS User's Manual for Revision 5.0*, Procedures Manual, ch. 5, Magnetic Analysis, Swanson Analysis Systems, Houston, PA, 1992.

Laure K. Lagorce received the engineering degree in physics of materials and a Master's degree in microelectronics from the Institut National des Sciences Appliquées (INSA), Toulouse, France, in 1994. As part of an exchange program between INSA and the Georgia Institute of Technology, Atlanta, she has pursued her research at the Georgia Institute of Technology from 1994 until 1997 and received the Ph.D. degree in 1997.

Her research interests included investigation of mechanical properties of materials using micromachined structures; development and characterization of magnetic materials; modeling, design, and fabrication of magnetic microactuators; and multichip modules (MCM). Currently, she is working as a Research Engineer at the Centre d'Elaboration de Materiaux et d'Etudes Structurales (CEMES-CNRS), Toulouse, France. Her research focuses on material characterization by X-ray diffraction.

Oliver Brand (M'97) received the diploma degree in physics from Technical University Karlsruhe, Germany, and the D.Sc. degree from ETH Zurich (Swiss Federal Institute of Technology), Switzerland, in 1990 and 1994, respectively.

From 1995 until 1997, he was a Postdoctoral Fellow with the Georgia Institute of Technology, Atlanta. In 1997, he joined the Physical Electronics Laboratory of ETH Zurich as Project Leader, Group Leader, and Lecturer. His research interest focuses on the development of microsensors and microactuators using industrial IC processes in combination with post-processing micromachining steps.

Mark G. Allen (M'89) received the B.A. degree in chemistry, the B.S.E. degree in chemical engineering, and the B.S.E. degree in electrical engineering, all from the University of Pennsylvania, Philadelphia, and the M.S. and Ph.D. degrees from the Massachusetts Institute of Technology (MIT), Cambridge.

Since 1989, he has been at the Georgia Institute of Technology, Atlanta, GA, where he currently holds the rank of Associate Professor. His research interests include micromachining fabrication technology, magnetic micromachined devices, and materials issues in micromachined structures and electronic packaging.

Dr. Allen was General Co-Chairman of the 1996 IEEE/ASME Microelectromechanical Systems Conference and is a Member of the Editorial Board of the *Journal of Micromechanics and Microengineering*.